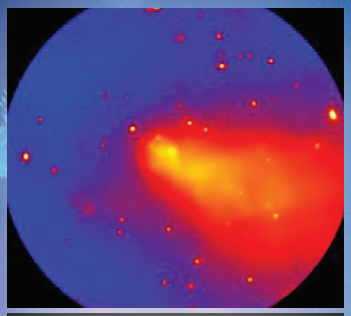

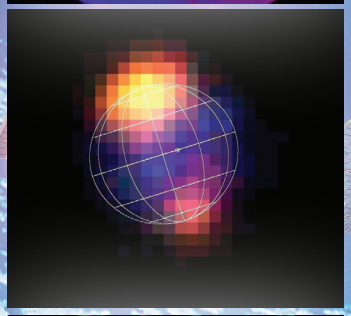

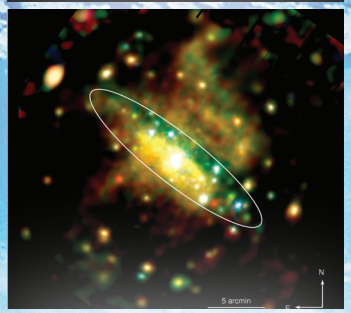

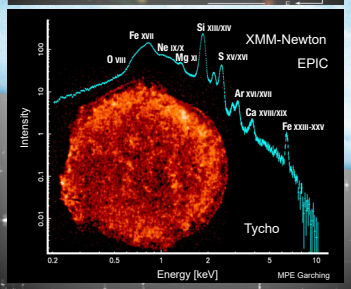

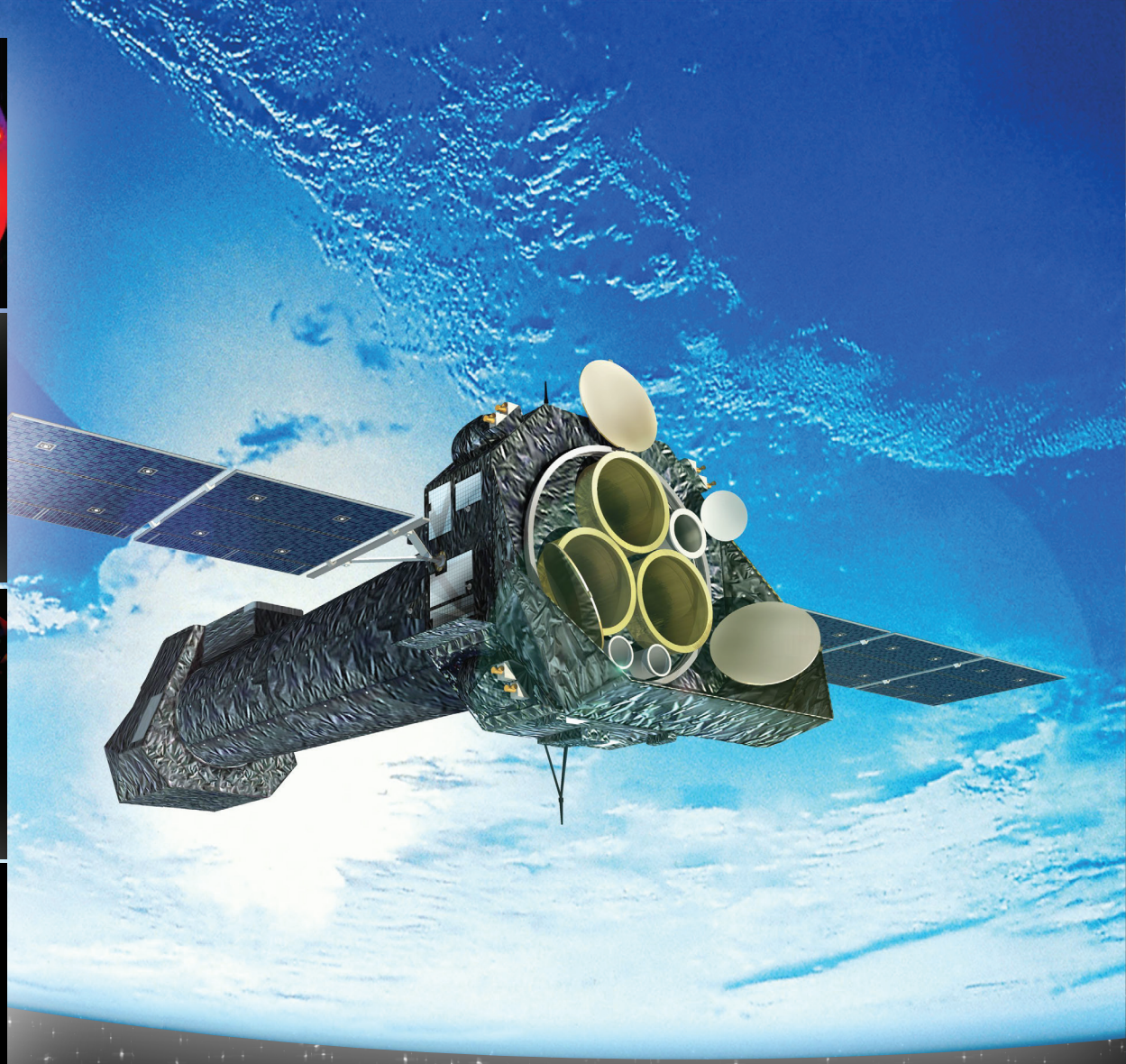

XMM-NEWTON
2019 SENIOR REVIEW PROPOSAL

XMM-Newton Guest Observer Facility (GOF), Guest Observer Funding, and the US Reflection Grating Spectrometer (RGS) Hardware Team

Prepared by: K. A. Weaver (NASA Project Scientist)
The US XMM-Newton Users Group (Jimmy Irwin, Chair)
Members: L. Brenneman, M. Gagne, M. Galeazzi, J. Halpern, U. Hwang, D. Lin, K. Kuntz, M. Sun, B. Williams, S. Snowden (Emeritus), and the staffs of the US XMM-Newton GOF and the US RGS Team

1.4 XMM-Newton Science 1
1.4.1 X-ray Background and Surveys 1
1.4.2 The problem of the Missing Baryons 2
1.4.3 Galaxy Clusters and Groups 3
1.4.4 Galaxies 5
1.4.5 Diffuse X-rays from the Milky Way 6
1.4.6 Transient Science: GRBs, TDEs, ULXs 8
1.4.7 Gravitational Wave (GW) science 10
1.4.8 Neutron Stars (NSs) 11
1.4.9 Active Galactic Nuclei (AGN) 13
1.4.10 Stars: Exoplanets, Star Formation, and Stellar Coronae 15
1.4.11 Supernovae/Supernova Remnants 16
1.4.12 The Solar System 17

1.4 XMM-Newton Science

In this section we focus on the breadth of XMM science discoveries from the last three years and we also consider where new observations may lead. **Of the large proposals accepted in the past four AOs, a steady ~75% have US participation**. These provide US astronomers with immediate access to a wealth of data.

Future science of XMM will be considerably enhanced by the well-calibrated and extensive X-ray source catalogs made available to the community. The 3XMM-DR8 catalog (Rosen *et al.* 2016) is the largest, and currently contains 775,000 X-ray detections of 531,000 individual sources. The X-ray Slew Catalog (2nd release) generated from over 2,100 slews (Saxton *et al.* 2008) now contains 29,400 sources. The XMM-OM Serendipitous Ultraviolet Source Survey (Page *et al.* 2012) last updated in 2017, contains 6.9 million detections from OM images, for 4.75 million unique sources.

XMM's extensive source catalogs are invaluable resources for for archival research, and they will grow in value as deeper, wide-field multiwavelength surveys become available for follow-up.

The continued development of the XMM Science Analysis System (SAS), improvements in calibration, and the advent of new software has made XMM analysis easier and more robust. The addition of new automatic data products also eases the study of large and complex data sets.

The following presents a summary of XMM science from the past three years. There is such a breadth of science that we cannot highlight everything. It is tempting to want to predict the many discoveries that will be made with XMM over the next three years. However, all XMM science is GO based and selected via competition. Also, NASA does not own or operate the satellite, or make proposal or telescope policy. The following studies will certainly lead to new science and recently-selected proposals make the best case for future discoveries. The references are coded here and throughout, where bold indicates a US lead author and green indicates a US co-author.

1.4.1 X-ray Background and Surveys

The XMM EPIC detectors are ideal for medium and shallow depth surveys with high legacy value. For example, the COSMOS field, acquired more than 10 years ago, still proves itself to be an astoundingly rich dataset, thanks to its multi-wavelength coverage and homogeneous 60 ksec coverage over 2 deg^2. In the past two years, more than 100 papers using those data have been published, covering a broad range of subjects, from galaxies to AGNs, clusters, and stars.

The XMM Slew Survey catalog provides a rich data set to be mined. It is only in the last two years that the full power of the Slew Survey has become available to the community. Fourteen years of data were released in XMMSL2 in March 2017. The survey covers 84% of the sky and we are only at the beginning of the full use of this catalog[6].

The XXL Survey (the Ultimate XMM Extragalactic Survey) was approved in 2010 as a VLP. This is the largest XMM observing program to date, with almost 7 Ms in about 540 observations. The survey consists of 2 fields of 25 deg^2 each (XXL-South and XXL-North – **Figure 6**) observed to a point source sensitivity of ~5×10^{-15} erg cm^{-2} s^{-1} (0.5–2 keV). Initial results from this survey were published in 13 papers in 2016 in a special issue of *A&A*, and a second special edition consisting of 20 papers was published in 2018, providing insight into X-ray ($z < 2$) cluster, ($z < 4$) active galactic nuclei (AGN), and cosmic background survey science. A deeper survey over the next decade is also being proposed, which, combined with deep multi-wavelength observations, will lead to solid standalone cosmological constraints and provide a wealth of information on the formation and evolution of AGN, clusters, and the X-ray background.

The 7 Msec XXL Program covering 50 deg^2 is producing dozens of papers ranging from high redshift galaxy clusters and AGN to cosmic background science, ultimately leading to stand-alone cosmological constraints.

As part of XMM AO-15, a 12 deg^2 survey at 50 ksec depth was also proposed and partially approved. This XMM-SERVS project consists of three of the most intensively studied regions on the sky, the XMM-LSS field, approved as part of AO-15, and the W-CDF-S and ELAIS-S1 fields approved in AO-17 ("Completing and Ensuring Major Impact from the XMM-SERVS Survey" [PI:Brandt]). XMM-LSS has now been fully observed and cataloged (Chen et~al. 2018), and W-CDF-S is now in the process of intensive observations. When completed, the XMM-SERVS survey will allow outstanding studies of ~ 12,000 AGNs and ~ 760 X-ray groups/clusters by powerfully leveraging multiple forefront intensive

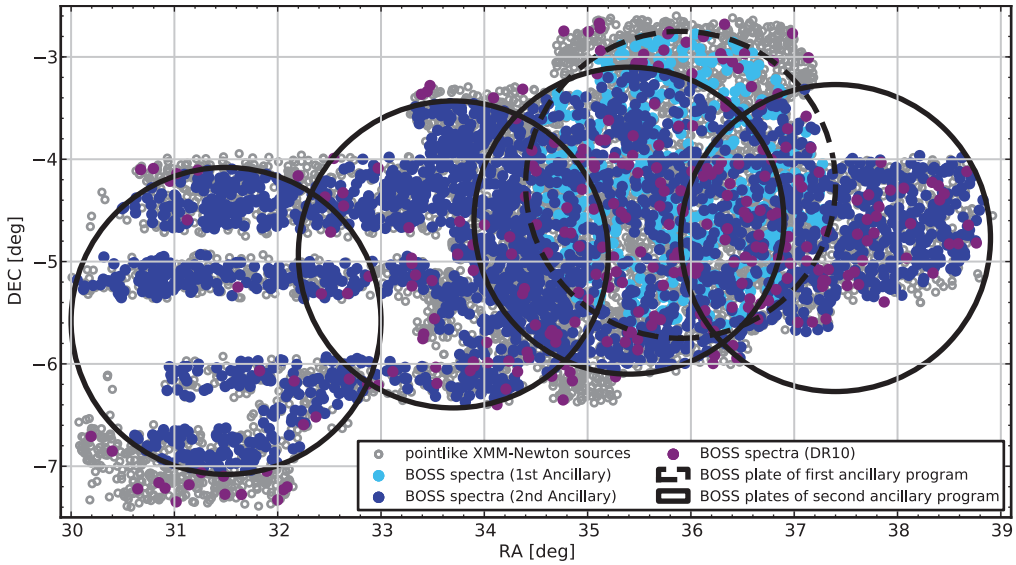

Figure 6. ***Large X-ray sky coverage.*** *XMM-XXL north with sky coordinates of XMM sources and targets with spectroscopic follow up (Menzel et al. 2016).* ***XXL provides by far the best view of the deep X-ray sky yet obtained****.*

radio-to-UV surveys: ATLAS, MIGHTEE, HerMES, SERVS, VIDEO, VEILS, DES, SUMIRE-HSC, PS1MD, VOICE, CSI, DEVILS, and PRIMUS. Aims are to advance dramatically studies of SMBH growth across the full range of cosmic environments (ranging from cosmic voids to clusters), links between SMBH accretion and star formation, exceptional AGNs at high redshifts, protoclusters, and multiple other topics. The targeted XMM- SERVS fields will have extraordinary legacy value as LSST/DES deep-drilling fields, VLT MOONS fields for massive spectroscopic follow-up, and prime TolTEC/ ALMA fields. They will also be targeted by the SDSS-V Black Hole Mapper and 4MOST surveys, which will perform intensive reverberation-mapping observations to measure SMBH masses directly.

Stripe 82 is a 31 deg^2 survey with depth up to 5–7.5 ksec and median flux limit of 5.4×10^{-15} erg cm^{-2} s^{-1}. More than 30 papers on this field were published in the past two years, focusing, among other things, on quasars, luminous AGNs, groups and clusters. For example, in a search for reddened AGN candidates, **LaMassa** *et al.* (2017) find that reddened broad-line AGNs are consistent with a transitory phase in AGN evolution as described by the major merger model for black hole growth. The XMM 4.5 Msec data toward the Chandra Deep Field South has also been highly productive, with papers on the search for the 3.5 keV line potentially associated with sterile neutrinos, AGN variability, and obscured AGNs.

Future Research: At this point, many XMM surveys provide incremental advances, as the observing time is adding to what has already been performed. But even incremental advances explore new parameters, either in the depth of the observations or in solid angle, opening the possibility of new discoveries. In many ways, the exciting portion of additional surveys is the discovery of the unknown, which could potentially open the door to new classes of objects, new physics, etc.

1.4.2 The problem of the Missing Baryons

One of the most intriguing endeavors in X-ray astrophysics has been the search for the missing baryons in the universe. We know that the visible baryonic mass of the Galaxy is factors of 2.5 to 5 smaller than that predicted by standard cosmological models. It is a strong possibility that the missing baryons are in the form of hot gas in the Galactic halo.

Both Nicastro *et al.* (2016a) and Gatuzz & Churazov (2018) have studied the Galactic ISM with the RGS, via absorption lines in the spectra of bright Galactic sources (XRBs) and extragalactic sources. Using either only low ionization lines (OI, OII) or the entire range of ionization states accessible between 10 and 30Å, they determined the mean ionization fractions, metallicities, and Doppler parameters in both the Galactic disk and the halo. Nicastro *et al* (2016b) have fit a joint disk+halo model to a similar collection of archival RGS measurements of OVII lines of sight and found that the best fitting models required a 6 kpc central “cavity”

in the halo. They attribute the cavity to nuclear activity 6 Myr ago and note that this model "closes the Milky Way baryon census". **If this result is correct, the hot gas in the halo solves the long-standing missing baryon problem in the Milky Way.** Conversely, Li & Bregman (2017), derive a lower halo mass from these data of 3–4×10^{10} $M_\odot$ rather than the 1.6–3.2×10^{11} $M_\odot$ required to close the mass problem. This is obviously a hot debate and further XMM data, both in absorption and in emission, are required to solve this issue.

An absorption line XMM study has made a tentative detection of the long-sought after Warm-Hot Intergalactic Medium responsible for a significant fraction of the missing baryons.

More recently, in 2018, Nicastro *et al.* claim to have conclusively detected the missing baryons via the WHIM. By using 1.75 Msec of exposure with the RGS instrument toward the X-ray brightest z>0.4 blazar 1ES 1553+113, these authors find two absorption lines attributed to O VII at a redshift of 0.4339 and 0.3551, with a sensitivity of 4.1–4.7σ and 3.7–4.2σ respectively (**Figure 7**). While a different origin for the lines is not completely ruled out, the missing baryon origin is supported by available multi-wavelength data.

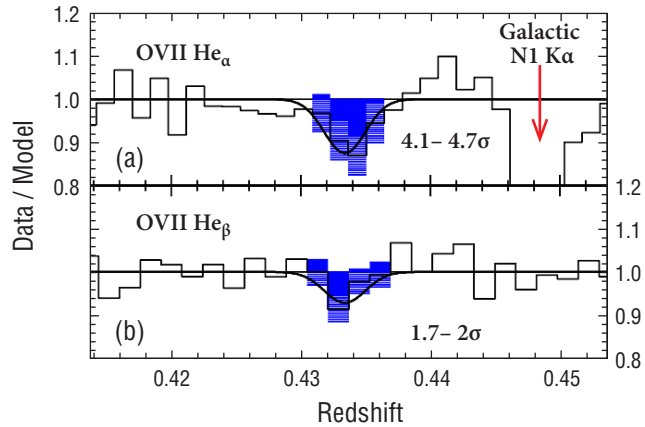

Figure 7. ***Detecting the Warm-Hot Intergalactic Medium (WHIM).*** *Ratios of XMM RGS1+RGS2 data of the blazar 1ES1553+113 with their local best-fitting continuum model, showing the two OVII He-α (top) and He-β (bottom) absorption lines believed to be from the WHIM (*Nicastro *et al. 2018).*

1.4.3 Galaxy Clusters and Groups

Surveys: The XMM XXL survey has begun to release their results from 2016 (Paper I: Pierre *et al.* 2016), with 36 papers already published by the end of 2018, including a sample of 365 galaxy clusters at z=0−1.2 (Adami *et al.* 2018). XXL also discovered the most distant X-ray selected cluster known at z~2 (**Mantz** *et al.* 2018; **Figure 8**). XMM is now the only X-ray telescope capable of efficiently detecting the hot gas of distant z>2 galaxy clusters in the Universe because such emission is redshifted into the soft XMM band. The X-ray mass in clusters is ~6 times the galaxy mass and so X-ray selection is crucial to study the earliest dominant baryonic mass components and selecting the most orga-

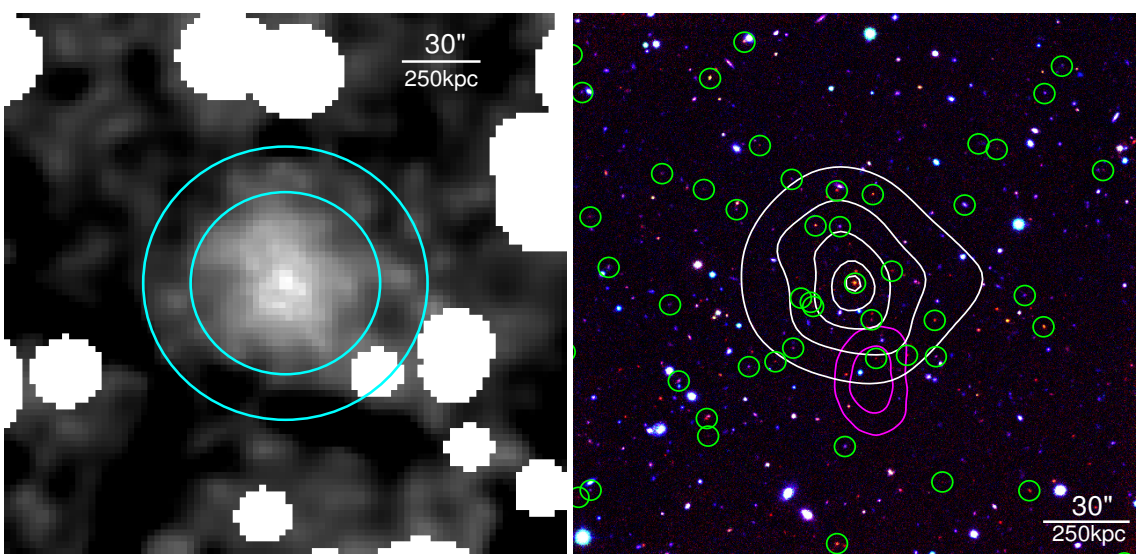

Figure 8. ***The highest redshift X-ray-selected cluster known to date.*** *(Left) Adaptively-smoothed XMM image of z=2 cluster XLSSC 122. (Right) iJK image showing XMM contours in white, offset CARMA S-Z contours in magenta, and photo-z members of the cluster inside green circles (***Mantz** *et al. 2018).* ***This way of finding high-z clusters is important because it selects a different kind of cluster—the most organized clusters****.*

nized clusters. With more completed surveys, XMM is expected to find many more high-z clusters. The XXL results have also been combined with weak lensing results to constrain the mass−temperature relation, further constraining the hydrostatic equilibrium mass bias (**Lieu** *et al.* 2016). **XXL cluster number counts have been used to constrain cosmological parameters (Pacaud *et al*. 2018) and future analysis can reduce uncertainties by a factor of three**.

XMM is now the *only* X-ray telescope capable of efficiently characterizing the hot gas of distant z>2 galaxy clusters in the Universe.

Scaling relations: Using XMM to observe optically-selected groups in the Complete Local-volume Groups Sample (CLoGS), **O'Sullivan** *et al.* (2017, 2018) showed that previous X-ray surveys have missed a significant number of nearby groups, primarily those systems which are disturbed by strong AGN outbursts or recent mergers, and those which lack cooling flows. XMM continues to play an important role in establishing scaling relations between X-ray observables and optical mass proxies from optical surveys (*e.g.,* DES — **Rykoff** *et al.* 2016; HSC survey — Oguri *et al.* 2018), or S-Z mass proxies from S-Z surveys (*e.g.,* SPT — Chiu *et al.* 2016, **McDonald** *et al.* 2016, **Bulbul** *et al.* 2018; CSO — **Sayers** *et al.* 2016).

ICM enrichment: XMM provides the highest quality X-ray measurements of the abundance of heavy elements, due to its large effective area, which further constrains SN models and ICM enrichment history. Abundance measurements require a lot of counts and so XMM's large area is key. Chandra can no longer constrain O abundance (lines at < 0.8 keV), or iron L-shell for a kT < 2 keV plasma. Mernier *et al.* (2016) studied the XMM RGS and EPIC data of the CHEmical Enrichment RGS Sample (CHEERS) of 44 cool-core galaxy clusters, groups, and elliptical galaxies. Their results suggest contributions from delayed-detonation SNIa and likely contribution from "Ca-rich gap transient" SNe. de Plaa *et al.* (2017) focused on the O abundance from CHEERS. These authors find a lack of dependence of O/Fe on temperature, which suggests that the enrichment of the ICM does not depend on cluster mass and that most of the enrichment likely took place before the ICM was formed.

With the loss of Hitomi, XMM/RGS is the *only* instrument capable of characterizing turbulence in the hot gas of galaxy clusters until at least 2021. The XMM large EA, spectral resolution and high dispersion uniquely enable this.

ICM dynamical state & turbulence: **Lovisari** *et al.* (2017) used XMM data of the Planck Early S-Z (ESZ) sample (148 clusters) to study the ICM morphology and confirmed that ESZ clusters tend to be more disturbed than X-ray selected clusters. Eckert *et al.* (2017) used the observed ICM density fluctuations to constrain the turbulent velocity and found that the derived turbulent energy rate is nearly proportional to the radio power of cluster radio halos, which supports the turbulent re-acceleration model for radio halos. **XMM/RGS continues to be the only instrument capable of studying the ICM turbulence in cool cores**. Applying line broadening and resonance scattering methods to RGS data, **Ogorzalek** *et al.* (2017, Stanford PhD dissertation) derived the best-known constraints for turbulent velocities in the hot gas of a sample of 13 nearby giant elliptical galaxies. The inferred turbulent velocity is too low to propagate energy radially to the cooling radius of the clusters within the required cooling time. The suggestion of suppressed turbulence implies some sort of dissipative force. Larger XMM RGS samples can search for the cause.

Other results: XMM continues to confirm high-z clusters, *e.g.,* a recent one at z = 2.506 (Wang *et al.* 2016). Note for such high-z and relatively soft X-ray sources, XMM is much more sensitive than Chandra (at z=2.5 and with kT=2 keV, the XMM count rate is 20 times higher in the 0.4–3 keV band than Chandra). Empasizing the power of XMM's large FOV, mosaic observations have revealed four sloshing cold fronts spanning over two orders of magnitude in radius in the Fornax Cluster (**Su** *et al.* 2017; **Figure 9**). XMM follow-up of a sample of star-forming brightest cluster galaxies (BCGs) reveal the first conclusive evidence that a super luminous disk galaxy is the central BCG of a galaxy cluster (**Bogdan** *et al.* 2018).

Future Cluster Research: Bartalucci *et al.* (2017) studied five z~1 clusters by optimally combining XMM and Chandra data, leveraging the throughput of XMM to obtain spatially-resolved spectroscopy and the spatial resolution of Chandra to probe the bright inner parts and to detect embedded point

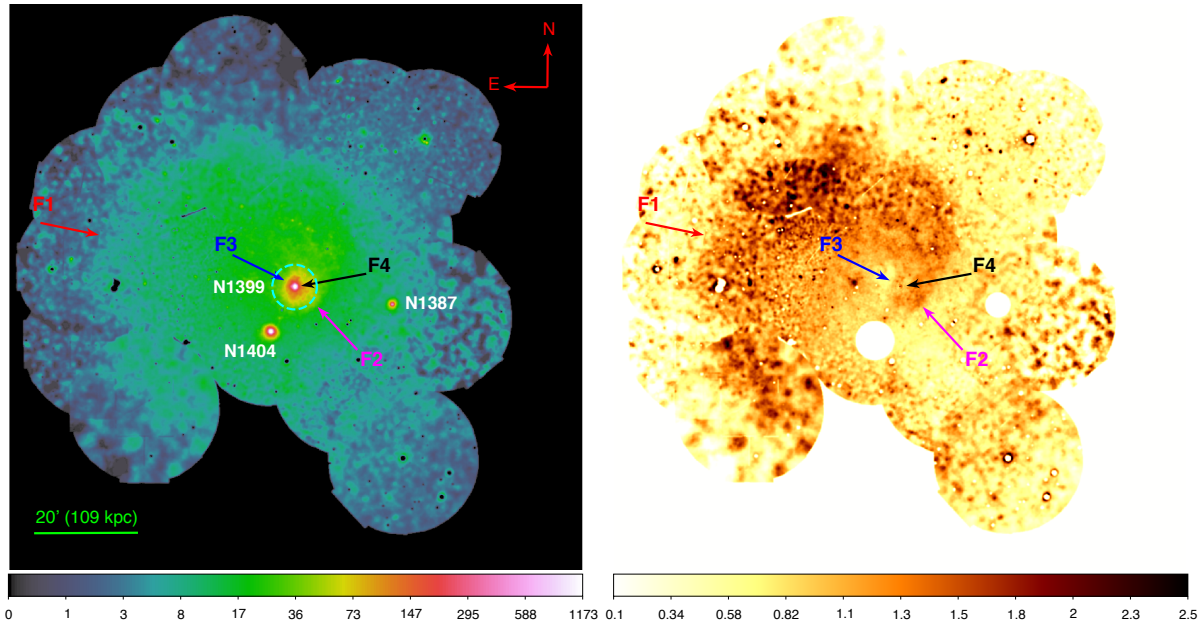

Figure 9. ***Key science enabled by the GOF's software development.*** *Exposure-corrected XMM mosaic of the Fornax cluster (left) and residual map (right) from* **Su** *et al. (2017) illustrating four sloshing cold fronts (marked F1-4) in one of our nearest cluster neighbors. The detection of cold front F1 (a large-scale structure to the NE) depended on XMM's FOV. Note that these images were created using the ESAS (***§2.2.2***), produced and supported by the US XMM GOF.*

sources. This work pioneers methods for future cluster research with XMM. A technique with the EPIC-pn Cu background line has recently been applied to constrain line velocities to 100 km/s (Sanders *et al.* "ICM Physics and Modelling Conference" at MPA, October 2018, "Snowcluster 2018 Conference" at Snowbird, Utah, March 2018), and will be tested on XMM VLP data of the Centaurus cluster, Virgo cluster and other clusters.

Constraining line velocities in clusters to 100 km/s opens a new direction of research with XMM and provides path-finding data for XRISM.

One of two AO-17 XMM Heritage programs will create a large, unbiased, signal-to-noise limited sample of galaxy clusters detected by Planck (PI: Arnaud) to address significant questions on cluster cosmology and baryon physics like non-gravitational heating and non-thermal pressure. The results will build the foundation for next-generation surveys like eROSITA. There are also proposals to finish a complete, local-volume galaxy group sample (PI: O'Sullivan) and to constrain the ICM abundance at two distant galaxy clusters (PI: Mantz).

1.4.4 Galaxies

XMM observations continue to enable groundbreaking discoveries about populations of X-ray sources in other galaxies. Among these observations were results from large programs on M31 and M33 (Sasaki *et al.* 2018, **Garofali** *et al.* 2018), including a dissertation concerning the M33 supernova remnant and high-mass X-ray binary populations (Garofoli *et al.* 2017, 2018). In M31, the latest deep XMM data have covered a large fraction of the area surveyed by the 824-orbit multi-cycle HST campaign (**Williams** *et al.* 2014) providing high-quality X-ray spectroscopy for many sources as well as for the hot interstellar gas (Sasaki *et al.* 2018). The spectroscopy yields a measurement of the amount of absorption present between us and each source, which is larger in the case of background sources. Because M31 is so large on the sky, over half of the sources detected are actually background galaxies, which can now be identified both through their high absorption and their optical counterpart candidates.

XMM LP programs of M31 and M33 use XMM's large FOV to enable an extensive study of the X-ray binary and supernova remnant populations of two of our nearest galactic neighbors.

The combination of XMM and NuSTAR has put tight constraints on the nature of accreting objects in nearby galaxies. Repeated observations of M33 X-8, the nearest ultraluminous X-ray source (ULX), show no clear support for a black hole as the com-

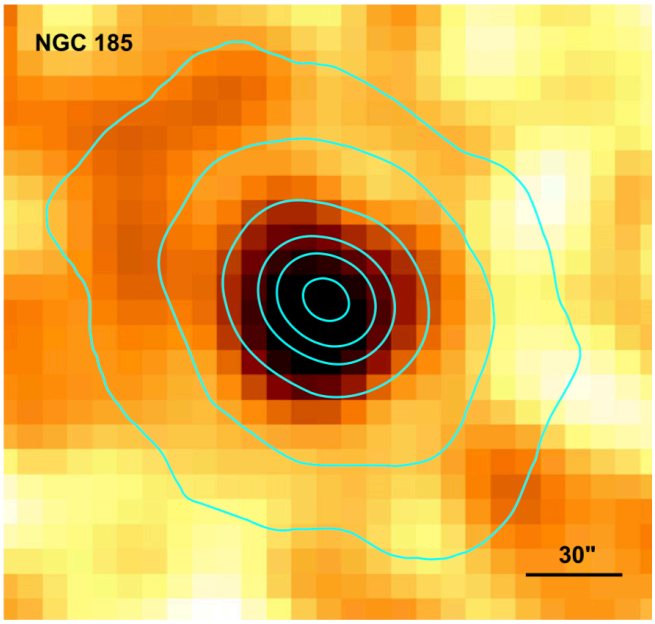

Figure 10. ***Old Stellar Populations.*** *Smoothed, combined XMM pn, MOS1, and MOS2 images of the 0.5–2 keV unresolved emission in NGC 185, overlaid by 2MASS Ks-band intensity contours. The 30" scale bar corresponds to a liner scale of ~90 pc (Ge et al. 2015).*

pact object (**West** *et al.* 2018). **Fürst** *et al.* (2016a) applied data from both observatories to determine the nature of the high energy emission from Centaurus A, finding tha it is most likely generated from an advection dominated accretion flow.

XMM observations played a critical role in the temperature, accretion state and variability measurements of the soft ULX in the bulgeless spiral NGC 247 (Feng *et al.* 2016), where a supergiant companion appears to be orbiting a high stellar mass ~30–50 $M_\odot$ black hole. This object is one of the softest ULXs known, and shows strong evidence for outflows from supercritical accretion. **XMM ULX data provide some of the best observational constraints available for models of stellar mass black hole accretion**.

The large previously published XMM survey of the Small Magellanic Cloud (SMC) continues to produce remarkable science, as there is now a complementary Chandra survey. The combination allows detailed spectral and timing long-term variability characteristics of the many bright X-ray sources in the SMC, all of which appear to exhibit pulsations (**Hong** *et al.* 2017). XMM also provides sensitive measurements of the X-ray emission from old stellar populations in local dwarf elliptical galaxies, such as NGC 185 (see **Figure 10**; Ge *et al.* 2015). Precise knowledge of X-rays from old stellar populations is crucial, not only for understanding stellar astrophysics, but for disentangling and quantifying the thermal emission from diffuse hot gas in nearby galaxies. These precision measurements can be used to calibrate the emission produced from old populations alone, enabling the separation of gas from stellar emission in more distant and complex systems.

Furthering the conversation over the "missing baryons," XMM detections of the circumgalactic medium of massive spirals have recently put tight constraints on the baryonic mass within the virial radius of galaxy halos, suggesting they are not sufficient to account for the missing baryons (**Figure 11**; **Li** *et al.* 2017, 2018a). This work was done by using XMM to achieve an unprecedented sensitivity for detecting low-surface brightness circumgalactic emission.

The high soft X-ray sensitivity of XMM is crucial for studying both the hot gas of galaxy groups and the circumgalactic gas around massive spiral galaxies.

1.4.5 Diffuse X-rays from the Milky Way

The principal issues concerning the hot, X-ray emitting ISM in the Milky Way, both disk and halo, are the amount of mass and energy in the hot gas. Much attention has turned to the ISM at the center of the Galaxy and the question of strong AGN activity in the past. Since the emission is diffuse, the answers rely on the distance to the emission, and thus on the quality of our cartography. However, X-ray studies are not limited to hot gas. These can constrain the distribution and nature of dust and, through absorption line spectroscopy, can address the distribution of gas in all states.

Cartography (the Galactic Center): Repeated observations of the Galactic center have revealed light echoes due to past activity by Sgr A*. Several groups have used the long baseline of XMM observations to map the light echoes, determine the dates of the activity that they are reflecting, and have used them to map the molecular clouds in the central molecular zone of the Galactic center (Chuard *et al.* 2018; Churazov *et al.* 2017). Coordinated NuSTAR observations show that the reflected continuum spectrum is a power law extending to at least 40 keV, consistent with Sgr A* outburst spectra (Krivonos *et al.* 2017).

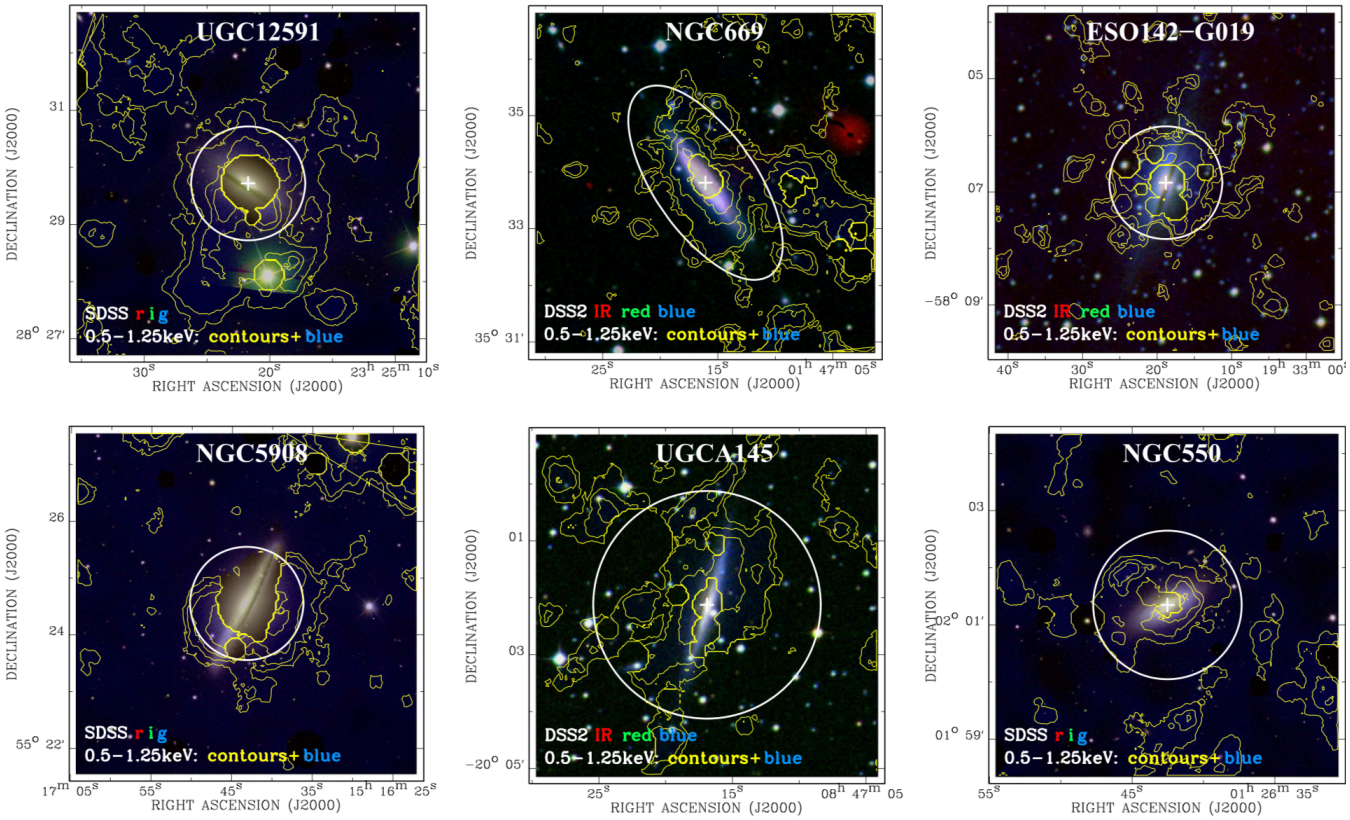

Figure 11. ***Missing Baryons?*** *XMM X-ray contours overlaid on the DSS or SDSS optical tri-color images of the central 6'x6' of the sample galaxies, showing circumgalactic X-ray gas around massive spirals. Contours are the diffuse soft X-ray images at different rms noise levels above the background (***Li** *et al. 2017).*

X-ray light echoes from previous outbursts of Sgr A* enabled by XMM's long baseline provide evidence of an active past for the Milky Way's supermassive black hole.

Cartography (the North Polar Spur (NPS)): The NPS is a bright, roughly circular, X-ray/radio continuum/HI feature with a radius of ~45°. It has been modeled both as a nearby (130 pc) superbubble blown by the Sco-Cen OB associations and as the result of AGN activity at the Galactic center. Although it may be the superposition of multiple X-ray structures related to different structures seen at other energies, the key to understanding the NPS is its distance(s). Lallement *et al.* (2016) executed a Large Program of observations of the low Galactic latitude end of the NPS to show that it must be >300 pc away, but were unable to place an upper limit. In the process they used the X-ray observations to strongly constrain the N(H2)/W(CO) conversion factor in this direction to $<10^{20}$ cm^{-2} K^{-1} km^{-1} s, which is significantly less than the typically cited Galaxy-wide value of 1.8×10^{20} cm^{-2} K^{-1} km^{-1} s. Thus, while mapping the Galaxy, these observations have contributed to understanding another controversial issue.

While it is increasingly difficult to associate the high-latitude portion of the NPS with the Fermi bubbles, the relationship at lower latitudes is also unclear. **Miller & Bregman** (2016) made an exhaustive study of the OVII/OVIII emission in the direction of the Fermi bubbles that showed that the region in the bubbles is hotter than the Galactic halo, and while lines of sight containing that hot gas are concentrated around the Galactic center, they are not confined to within the Fermi bubble outlines. The wide field of view and soft response of the EPIC make XMM the only instrument that can pursue these studies.

Transient X-ray sources produce multiple rings (**Figure 12**) as their X-ray light transverse the Milky Way allowing us to use EPIC to precisely map the ISM of the Galaxy.

Cartography of the ISM with dust: Dust along the line of sight scatters X-rays; measuring the scattering halo around bright point sources allows one

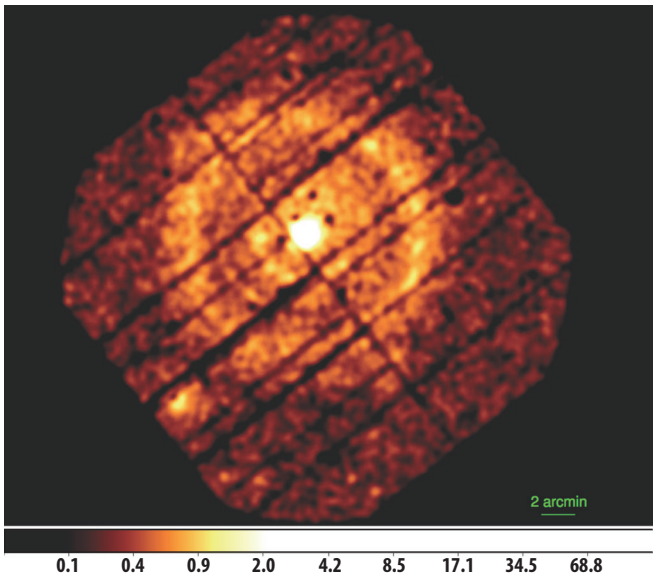

Figure 12. ***ISM dust properties inferred from X-rays.*** *EPIC-pn image from* Pintore *et al. (2017) showing dust-scattering rings extending up to 9' around the GRB afterglow.*

to determine the location of the dust along the line of sight and to constrain the properties of the dust. X-ray fitting constrains the number and porosity of large dust grains, which are not well constrained by optical/UV methods. **Corrales** *et al.* (2016) have shown that not accounting for dust scattering (*i.e.,* using only photoelectric absorption models) can overestimate absorbing column densities by ~25% and underestimate fluxes by up to 50%, but the effect is often smaller (**Smith, Valencic, & Corrales** 2016).

Dust haloes from transient sources form expanding rings. From the rate of expansion one can measure the distance to the layers of dust. One of the most spectacular examples is that of GRB 160623A for which six separate dust layers were measured, allowing us to map the ISM in this direction "with extraordinary precision" (Pintore *et al.* 2017). As can be seen from **Figure 12**, this study was made possible by XMM's strong soft response and large field of view.

X-ray Shadows: Shadowing studies to determine the strength of the Galactic halo emission have been difficult due to the presence of solar wind charge exchange (SWCX), which adds a temporally variable component to the strong emission lines typically used as temperature diagnostics (such as OVII and OVIII). XMM's mosaicking observation mode may allow the SWCX emission to be accounted for.

Mosaicking: By removing the need to repeat the same instrumental setup over a series of short observations, XMM's mosaicking mode allows very efficient imaging of extended regions. A member of the GOF recently realized that the same mode could be used to interleave multiple observations of a pair of targets in order to remove time variable foreground emission due to the SWCX. Testing of this method will be done this year.

1.4.6 Transient Science: GRBs, TDEs, ULXs

Gamma-Ray bursts (GRBs): XMM's sensitivity enables the study of GRB afterglows to faint limits, which probes the geometries and environments of their explosions. The exceptional GRB 130427A was the brightest gamma-ray burst detected in 30 years, with an isotropic-equivalent fluence of 8.5×10^{53} ergs at z = 0.34. Its afterglow was detected in X-rays for an unprecedented 2.7 years (De Pasquale *et al.* 2016). The surprising result is that the flux followed a single power law in time, $t^{-\alpha}$ with α=1.309±0.007. The absence of a "jet break" due to the slowing or expanding of the collimated outflow places extreme (implausible) limits on all of the parameters involved in standard forward shock models. The ISM density must be low ($n\leq10^{-3}$ cm^{-3}) and the initial Lorentz factor and beaming-corrected energy must be high (Γ_0 > 1500, E $\approx10^{52}$ ergs). No transition is seen from a stellar wind density profile to a uniform ISM, and the very low density required is difficult to reconcile with its location in the host galaxy and significant absorption at the redshift of the burst. One popular hypothesis for the GRB central engine, a newly born, rapidly spinning magnetar, is difficult to reconcile with the required energy, which seems instead to require a black-hole driven jet, if such a model can work at all.

XMM has discovered or followed up on several unusual tidal disruption events of stars by both supermassive and intermediate-mass black holes at the centers of galaxies.

Tidal disruption events of stars (TDEs) by massive black holes: XMM pointed observations are frequently used to follow up TDEs discovered from the slew observations. **Lin** *et al.* (2017) found a decade-long super-Eddington accreting TDE from the 3XMM-DR5 SSSC. The host is a dwarf starburst galaxy at a distance of 689 Mpc. After an apparently fast rise within ~4 months detected by XMM, the X-ray luminosity decayed only slightly and has been persistently high at around

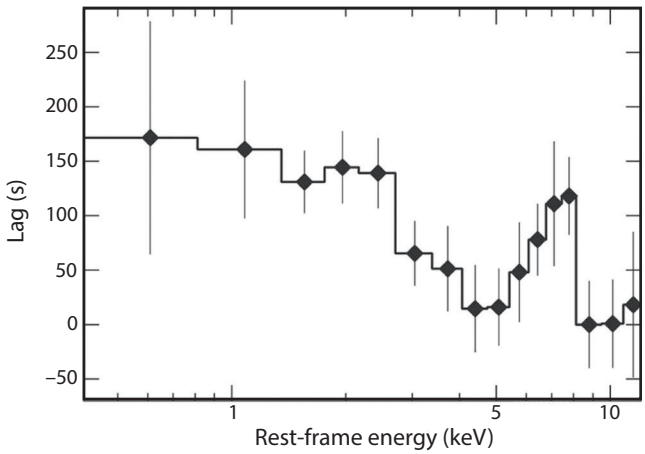

Figure 13. ***Peering within 10 gravitational radii of a tidal disruption event.*** *The lag-energy spectrum of the TDE Swift J1644+57 using an XMM observation indicating that the iron Kα emission line is gravitationally redshifted (***Kara** *et al. 2016).*

the Eddington limit for a decade. **The long decay and the X-ray spectrum suggest a TDE of an unusually long super-Eddington accretion phase that has never been observed before**. The whole event could be explained as a full disruption of a $2M_\odot$ star by a 10^6 $M_\odot$ black hole.

Lin *et al.* (2018) found the best evidence thus far that an intermediate-mass black hole (IMBH) could be detected in a TDE. The IMBH resides in a compact star cluster of stellar mass ~10^7 $M_\odot$ and effective radius <20 pc, at a projected distance of 12.5 kpc from the center of a large lenticular galaxy at 247 Mpc. XMM, Chandra and Swift observations from 2006–2016 show an X-ray outburst with the luminosity systematically decreasing by an order of magnitude from 1.1×10^{43} erg s^{-1} to 1.1×10^{42} erg s^{-1}. The decay is consistent with the standard TDE model of $t^{-5/3}$, with the stellar disruption inferred to occur in mid-October of 2003. Based on X-ray spectral fits with a disk model, **Lin** *et al.* (2018) estimated the black hole mass to be around 5×10^4 $M_\odot$.

High-quality XMM data have enabled **Kara** *et al.* (2016) to observe reverberation arising from gravitationally redshifted iron Kα photons reflected off the inner accretion flow in the TDE Swift J1644+57. These authors calculated the lag-energy spectrum of the event using an XMM observation on April 16th, 2011 and found that 5.5–8 keV rest-frame emission is delayed by ~100 s relative to 4–5 keV and 8–13 keV emission (**Figure 13**). The profile of the line lag was asymmetric, indicating that the Iron Kα emission line is gravitationally redshifted from within 10 gravitational radii. The detection of reverberation from the relativistic depths of this event demonstrates that the X-rays do not arise from the relativistically moving regions of a jet, as previously thought.

Ultraluminous Off-nuclear X-ray Sources (ULXs): Important breakthroughs have been achieved in the last few years when coherent pulsations were detected in four ULXs using XMM and NuSTAR data, suggesting that a significant fraction of ULXs are accreting X-ray pulsars (ULX pulsars). **The discovery of ULX pulsars is an exciting result from the XMM EXTraS project (Exploring the X-ray Transient and variable Sky), which harvests the temporal domain information in the serendipitous data collected by the EPIC**.

Israel *et al.* (2017) discovered the brightest ULX pulsar known thus far in NGC 5907, with a peak X-ray luminosity of 10^{41} erg s^{-1}. They first discovered a coherent signal at a frequency of ~0.88 Hz from this extreme source in an XMM-Newton EPIC observation on July 9th, 2014. It has astonished observers that the ULX in NGC 5907, one of the best intermediate mass black hole candidates, is actually an accreting neutron star. Other properties of this system must also be extreme to sustain its apparent luminosity, 1000 times beyond its Eddington limit.

XMM was also used to discover the ULX pulsars NGC 7793 P13 and NGC 300 ULX1 (**Fürst** *et al.* 2016b; Carpano *et al.* 2018), and NGC 300 ULX1 (Maitra *et al.* 2019). Standard accretion models fail to explain their extreme luminosities, even assuming beamed emission. These findings suggest that other extreme ULXs might also harbor NSs, which is prime future work for XMM.

High-resolution RGS observations allowed Pinto *et al.* (2016) to detect highly blueshifted (~0.2c) absorption lines in ULXs NGC 1313 X-1 and NGC 5408 X-1. In NGC 1313 X-1, they also identified strong, rest-frame emission lines from a mixture of elements at varying degrees of ionization (**Figure 14**). The emission lines are highly significant and can be well-modeled with a rest-frame, collisional ionization equilibrium gas. Emission lines in both NGC1313 X-1 and NGC5408 X-1 are probably associated with collisional shock heating between the circumsystem gas and the outflowing wind that has been identified in the form of absorption lines. It seems that the accretion flow in some ULXs can be associated with powerful winds that leave their imprint in emission and absorption lines.

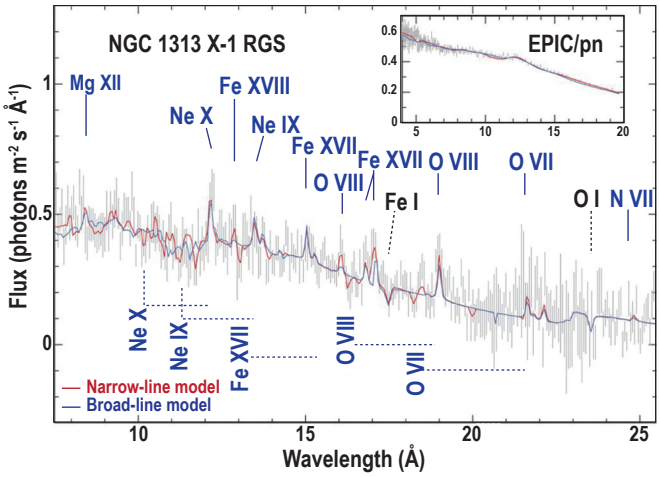

Figure 14. ***Outflowing winds from accretion flows.*** *Simultaneous spectral fits to the stacked XMM RGS (main panel) and EPIC/pn (inset) spectra of NGC1313 X-1 showing individual line species including O, Ne, and Fe easily resolved (Pinto et al. 2016).*

Future TDE research: Currently, the X-ray sample of TDEs is too small to constrain physical models. Therefore, an important task in the study of TDEs is to significantly enlarge the X-ray TDE sample by following up candidate TDEs detected in optical wavelengths and by searching archival data. Two XMM observations were approved in AO-17 to follow up two new TDE candidates discovered from the XMM SSSC with quasi-soft X-ray spectra, which is characteristic of super-Eddington accretion. The XMM follow-up observations will measure flux decay, which is needed to confirm the TDE nature of the events. New areas of TDE reseaerch include searching for super-Eddington accreting events, outflows, IMBHs, and QPOs.

Future ULX research: Our understanding of the nature of ULXs is far from complete. How do we distinguish between ULX pulsars, super-Eddington accreting black holes, and IMBH? In AO-16/17, XMM accepted 4 LP/VLP proposals in the field of ULX research. One is the study of high Eddington accretion with the ultrafast outflow of NGC 1313 ULX-1. Two LP/VLP proposals are for NGC 5907 ULX-1, with one to combine XMM and NuSTAR to obtain orbital- and spin-phase-resolved broadband X-ray spectroscopy of the object and the other to have a long look at the off state in order to determine the magnetic field in such an extreme object. Another VLP proposal was to triple the number of known ULXs where sensitive searches for X-ray pulsations and cyclotron features can be carried out.

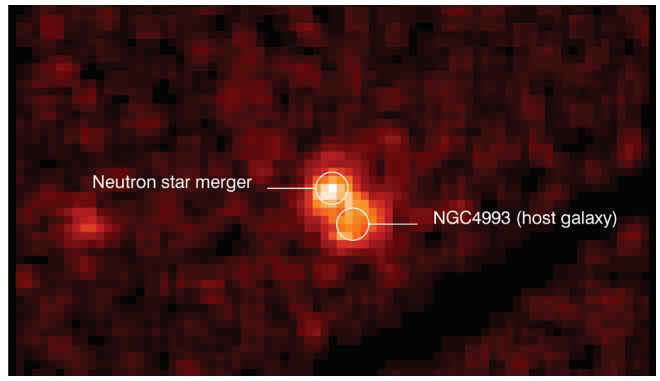

Figure 15. ***X-ray signature of a gravitational wave event.*** *An sGRB X-ray afterglow (D'Avanzo et al. 2016). The X-ray emission of GW170817 / GRB 170817A (upper circle, 4" radius) is clearly visible close to the nucleus of its host galaxy (lower circle). The image was obtained by co-adding the XMM pn and MOS.*

The XMM/RGS can detect highly blueshifted outflows (v ~ 0.2c) from Ultraluminous X-ray Sources.

1.4.7 Gravitational Wave (GW) science

XMM is poised to follow-up on gravitational wave events. A GW-event is expected to be accompanied by a short Gamma Ray Burst (sGRB) which produces afterglows from the IR through X-ray bands. GW170817-GRB170817A was the first observed GW-event of a NS-NS merger. The event was detected by LIGO/Virgo (GW 170817; **Abbott** *et al.* 2017), and subsequently found to be associated with the weak sGRB 170817A (**Goldstein** *et al.* 2017; Savchenko *et al.* 2017). The fact that an X-ray counterpart would be visible after several months was unexpected. D'Avanzo *et al.* (2018) report an observation of GRB 170817A, performed with XMM 135 d after the event (on 29 December, 2017; **Figure 15**) and find that the change in the temporal evolution of the light curve suggests either a structured jet or a jet-less isotropic fireball with stratification in its radial velocity structure.

Future GW research: XMM has begun a gravitational wave follow up program. After a LIGO/Virgo alert, the ToO is assessed against the XMM visibility window; the satellite can reach reaction times of ~6 hours. The AO-18 TAC has accepted several ToO proposals for or including GW-events and/or sGRBs. If X-ray counterparts are long-lived, then XMM will be able to observe the large majority of GW-event afterglows.

1.4.8 Neutron Stars (NSs)

The high-throughput spectroscopy and timing simultaneously available with the XMM EPIC cameras are needed to determine the physical properties of the majority of isolated pulsars that are radiatively inefficient at all wavelengths, and are often only detectable in X-rays. X-ray measured spin-down rates determine the pulsars' ages, dipole magnetic field strengths, and spin-down luminosity. The imaging and timing capabilities of XMM are also used to identify a large number of NS first detected, but not identified, at other wavelengths.

Central Compact Objects: The so-called central compact objects (CCOs) in SNRs are a class of ≈10 neutron stars that have soft thermal X-ray spectra and are undetected at any other wavelength. For the three CCOs in which pulsations have been detected, their small spin-down rate implies a surface dipole magnetic field strength of (3−10) x 10^{10} G, very weak for a young NS.

Recent work on CCOs has concentrated on understanding their spectra, which is now only possible with XMM's soft response. An intriguing proposal is that their apparent two-temperature blackbody or hydrogen atmospheres should be deprecated in favor of a single temperature carbon atmosphere model, which fits just as well and requires a reasonable NS radius. A single temperature could also explain why most of the CCOs have not been observed to pulse (Suleimanov *et al.* 2017). A carbon atmosphere was first proposed for the CCO in the Cas A SNR (Ho & Heinke 2009). As the youngest known NS, the Cas A CCO could be hot enough to burn hydrogen and helium to carbon. A carbon atmosphere has been advocated for XMM spectra of three more CCOs (Doroshenko *et al.* 2018; Klochkov *et al.* 2013, 2016).

Long-term timing with XMM and Chandra over 15 years recently discovered the first glitch in a CCO pulsar, 1E 1207.4−5209 (Gotthelf & Halpern 2018). Glitches are sudden increases in spin frequency that are thought to result from the unpinning and repinning of neutron superfluid vortices in the inner crust. But glitch activity correlates with spin-down rate, such that pulsars with spin-down rates as small as those of CCOs have never been seen to glitch. This event is therefore unexpected and unprecedented. The exact mechanism that triggers a glitch is unknown, but this behavior of a CCO is a unique piece of evidence that some property of a young NS, such as temperature or internal B-field, is implicated.

Long-term monitoring with XMM helped discover the first sudden increase in spin rate (a glitch) in a central compact object in a supernova remnant, which may shed light on the NS equation-of-state.

Millisecond Pulsars (MSPs): MSPs are an interesting new class of pulsar found with Fermi, but Fermi can't characterize them without XMM. These so-called "black widow" (BW) pulsars, with <0.1 $M_\odot$ companions, and "redbacks," with >0.1$M_\odot$ companions, are the end stages of the low-mass X-ray binary progenitors that spin the NS up to millisecond periods by accretion. Redbacks are nearly filling their Roche-lobes, while BWs companions are often significantly smaller.

XMM plays a key observational role in identifying these Fermi selected sources, especially ones that are not radio detected, by imaging their error circles and finding a source with orbital modulation or flaring, both of which are caused by interaction between a relativistic pulsar wind and the companion star. Fermi sources that were recently identified in this way using XMM are 3FGL J2039.6−5816 (Salvetti *et al.* 2015) and 3FGL J0838.8−2829 (**Halpern** *et al.* 2017; Rea *et al.* 2017). These are certainly redback MSPs, with orbital periods of 5.47 hr and 5.15 hr respectively, even though their pulsations have not yet been detected. PSR J1306−40, a radio-selected redback with a 26.3 hr orbit, was also detected by XMM (Linares 2018).

Bright flares in BWs and redbacks sometimes approach or exceed the spin-down power of the pulsar or typical flares in young M stars (An *et al.* 2017). Together with the flat power-law X-ray spectra, this suggests that magnetic reconnection, rather than diffusive shock acceleration, is responsible for energizing the synchrotron emitting electrons.

Using its multi-wavelength coverage, XMM was the first to detect a flare in a redback system simultaneously in X-ray and optical.

Of principal interest is the location and emission mechanism of the flares, whether in an intrabinary shock between the stellar winds, or in magnetic fields intrinsic to the companion. Future observations with the fast mode of the Optical Monitor can provide comparable time resolution to the X-rays, to determine the broad-band spectrum of the flares,

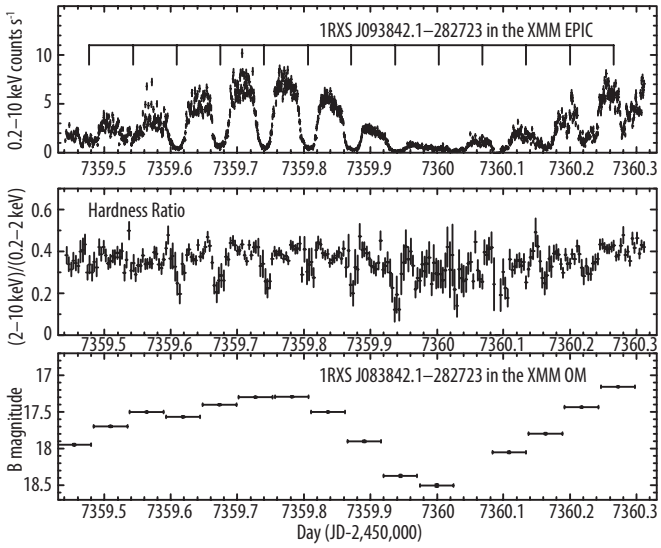

Figure 16. ***Light curve of 1RXS J083842.1−282723, the most asynchronous polar known****. Top: Combined EPIC pn and MOS broad-band light curve in 60 s bins. Middle: Hardness ratio of counts in 300 s bins. Bottom: XMM Optical Monitor magnitudes from 4400 s exposures in the B-band. This image from* **Halpern** *et al. (2017) illustrates XMM's ability to obtain simultaneous time-resolved X-ray fluxes, X-ray hardnesses, and optical fluxes.*

and test for any orbital phase dependence of flare occurrence.

Future Research: The XMM EPIC pn CCD will be used to identify, and study recycled pulsars in compact binaries that are waiting to be discovered among the unassociated Fermi sources. It is especially needed when the pulsar is obscured in radio, or is inherently radio quiet. The same capabilities apply to identifying young, energetic pulsars that are discovered as very high-energy gamma-ray sources by atmospheric and water Cherenkov telescopes, as many of these will host radio-quiet pulsars.

Cataclysmic Variables (CVs) and X-ray Binaries (XRBs)

Cataclysmic variables (CVs) are accreting binaries in which a dwarf star donates mass to a white dwarf (WD) via Roche-lobe overflow, and include strong magnetic field polars (AM Herculis stars), and weaker magnetic field intermediate polars (IPs, or DQ Herculis stars). With its capability for long, *uninterrupted* observations in X-ray and optical, XMM is uniquely able to identify period(s) of such binaries and characterize the large number of magnetic CVs discovered by hard X-ray surveys such as Swift/BAT and INTEGRAL/IBIS. **With periods of CVs usually in the range of minutes to several hours, the long, uninterrupted observations possible with XMM are essential to measure the periods, avoid aliasing, and discover eclipses**. In the latest results from a long-term program to study these sources using XMM, Bernardini *et al.* (2017, 2018) clarified the nature of eight more such CVs.

> Only XMM has the combined optical and X-ray sensitivity and long-stare capabilities required to make characterizing CVs routine.

An exciting new discovery with XMM involves the the half-dozen CVs called "asynchronous polars" (APs), in which the spin and orbit frequencies, ω and Ω, respectively, differ by 1–2%, rather than the expected identical frequencies. It is believed that nova eruptions perturb the spin period of the WD to create the asynchronism. Thus, APs probe the mass and angular momentum loss in nova explosions. Recently, using long observations with XMM, Rea *et al.* (2017) and **Halpern** *et al.* (2017) discovered that 1RXS J083842.1−28272 is such an extremely asynchronous polar. It has a strikingly simple light curve, which may prove useful in interpreting other, more complicated systems (**Figure 16**). The X-rays show a factor of 10 variation with a period of 94.6 minutes, interpreted as self-occultation of the accreting pole by the spinning WD, plus a broader modulation of the accretion rate itself on a timescale of ~0.6 day. There is also an optical spectroscopic period of 98.413±0.004 minutes, which is consistent with being the orbital period. At the minimum of the 0.6-day cycle, the phase of the spin oscillation jumps by ≈120°. This is the signature of pole-switching accretion. Assuming that there are two accreting magnetic poles 120° apart in azimuth, the 0.6-day variation represents $3(\omega-\Omega)$, and the asynchronism $(\omega-\Omega)/\Omega$ is 4%.

An even more extreme candidate is RX J0524+42 (Paloma), which has X-ray periods of 156 and 130 minutes, implying asynchronism of 17% (Joshi *et al.* 2016). It is not clear if such systems are polars, IPs, or pre-polars approaching synchronism for the first time. Such behavior is most easily recognized using the long, continuous observations, both X-ray and optical, that are possible with XMM. Satellites in low-earth orbit, and ground-based telescopes, are interrupted on time-scales similar to those of the CVs' periods, which severely handicaps them for these studies.

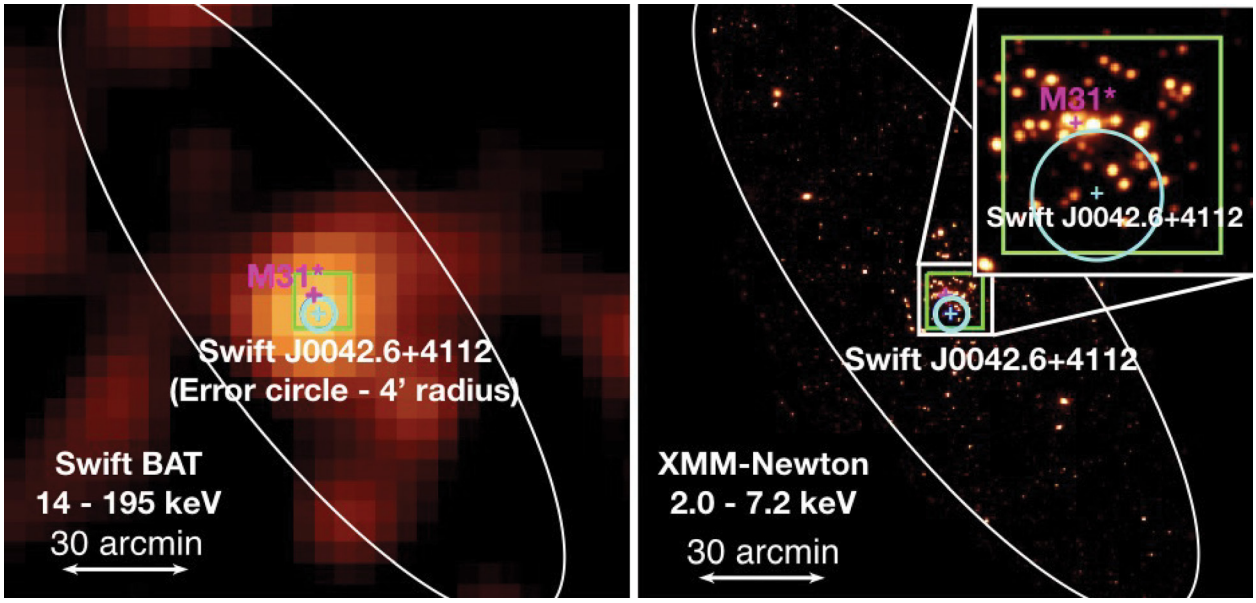

Figure 17. ***The most luminous dipping LMXB known.*** *Left: Swift BAT 14–195 keV image of M31. The ellipse shows the optical extent of M31. The magenta cross depicts the location of the nucleus, M31*. The blue plus sign indicates the location of Swift J0042.6+4112, with a 4' radius error circle. Right: XMM 2.0–7.2 keV image. The inset is the magnified view of the bulge region showing resolved point sources within the BAT error circle (blue), one of which turned out to be the newly discovered pulsar 3XMM J004232.1+411314 (***Yukita** *et al. 2017).* ***XMM was the only mission with the capability to confirm the pulsar nature of the source dominating the E>30 keV emission from M31****.*

A major recent discovery by XMM is a class of 'asynchronous polars', where the white dwarf binary spin and orbital frequencies of the system differ, suggesting nova eruptions.

The sensitivity and imaging capability of XMM enable it to discover and time accreting X-ray binary pulsars in local-group galaxies. Recently, XMM data was used in conjunction with data from Swift, Chandra, and NuSTAR to detect a pulsar in M31 (**Yukita** *et al.* 2017).

The identification of the LMXB pulsar in M31 with XMM represents the first time a pulsar has been seen at this distance.

Swift J0042.6+4112 is the most prominent hard X-ray source in the inner bulge of M31, 3.′7 from the center (**Figure 17**). Its precise nature was unknown until Marelli *et al.* (2017) studied the light curves of 0.8 Ms of archival XMM data on 3XMM J004232.1+411314, which revealed multiple dips in the light curve with a period of 4.01 hr. Thus, it is the most luminous dipping LMXB known, with L_X=(0.8−2.8)×10^{38} erg s^{-1}. **It took the combination of BAT-NuSTAR-Chandra to pinpoint the source, but XMM timing was required to identify it**. Variability studies with the pn (Rodríguez Castillo *et al.* 2018) discovered a 3 sec. spin period, and pulse timing confirmed an orbital period of 4.2 hr. The mass of the companion is thus estimated at 0.2–0.3 $M_\odot$. Transient behavior in the L_X detected in the future would would allow a test of magnetic field strength. This is a prime example of how the unique combination of high throughput, spatial resolution, and timing ability of XMM is still needed to extend the study of (even the brightest) X-ray binaries as far away as M31. Such systems can span a more extreme range of properties than the Milky Way's neutron star binaries.

XMM's unique combination of high throughput, spatial resolution and timing ability make it indispensible for studying X-ray pulsars in other galaxies.

1.4.9 Active Galactic Nuclei (AGN)

AGN science continues to be a cornerstone of XMM's portfolio. The simultaneous data collected by the EPIC, RGS, and OM enable astronomers to examine the properties of the absorbing gas/outflowing wind, continuum, distant and inner-disk reflection, and soft excess self-consistently.

Accretion processes: Recently a number of observational programs (*e.g.,* NGC 5548 with Swift) have shown that the UV/optical variations in AGN

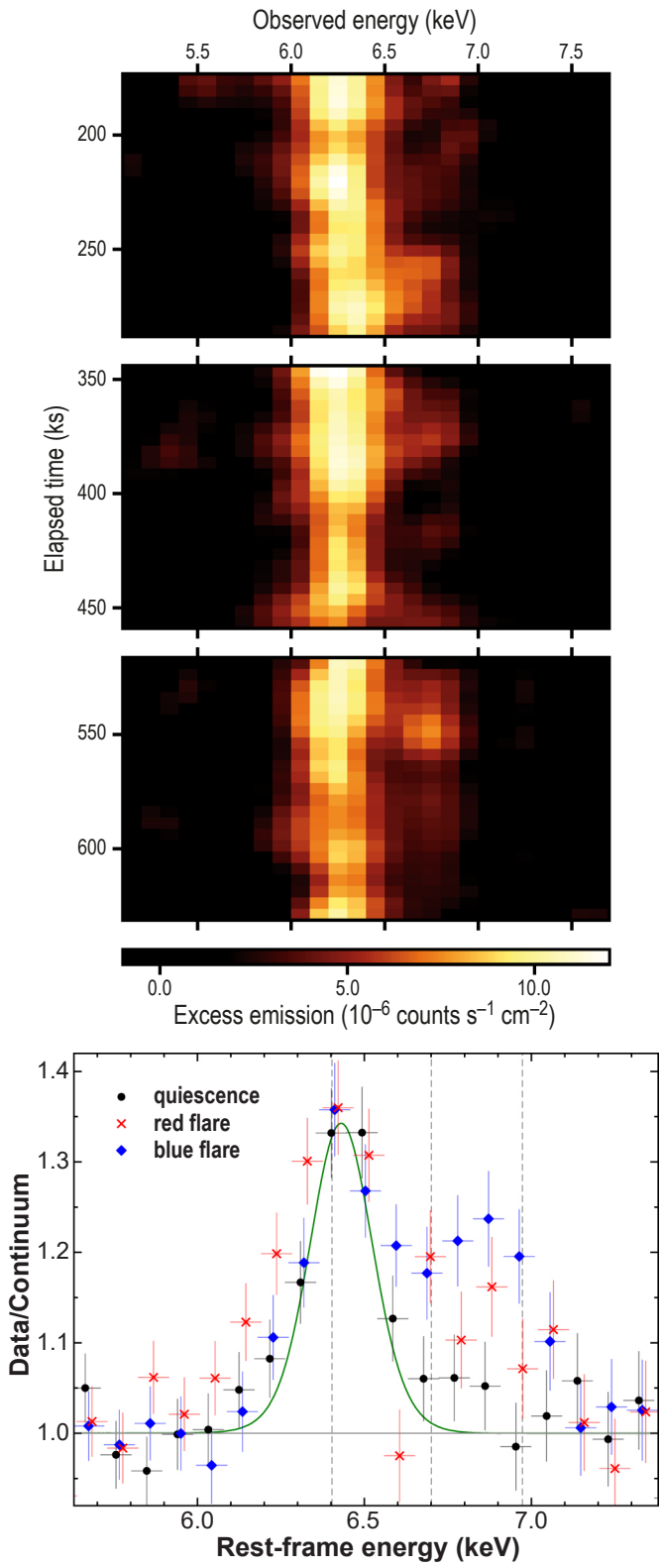

lag behind the X-ray variations in a manner strongly supportive of X-ray reprocessing. Somewhat surprisingly, the implied size of the accretion disk in this case is ~3x greater than expected from a standard, smooth, Shakura-Sunyaev thin disk model. Although the difference may be explained by a clumpy accretion disk, it is not clear whether the difference will occur in all AGN or whether it may change as, *e.g.,* a function of black hole mass, accretion rate or disk temperature. McHardy *et al.* (2016) investigated the origin of short timescale (weeks/months) variability of AGN through these X-ray and UV time lags, specifically looking at intrinsic disk variations and the reprocessing of X-ray emission by a surrounding accretion disk as underlying causes of these lags. For low mass ($M_{BH} < 10^6$ $M_\odot$) AGN, the combination of XMM/EPIC (X-rays) with the OM in fast readout mode allows an X-ray/UV-optical lag to be measured within a single long observation. In NGC 4395, the authors found that the UVW1 flux (effective wavelength = 2900 Å) lags the X-rays by ~470 s. Simultaneous observations at six different ground-based observatories also allowed the g-band lag (~800 s) to be measured. These observations are in agreement with the X-ray reprocessing scenario.

With it's unique combination of instruments, XMM can obtain the crucially-needed simultaneous X-ray/optical light curves of AGN to search for time lags, indicative of X-ray reprocessing.

Relativistic phenomena close to the event horizon: Nardini *et al.* (2016) reported on a large observing campaign on the bare Seyfert galaxy Ark 120, jointly carried out in 2014 with XMM, Chandra and NuSTAR. The sensitivity of the EPIC-pn spectra were critical in identifying excess emission detected on both sides of the narrow Fe Kα line. The red wing emission component (6.0–6.3 keV) clearly varies in strength in about one year, and hints at the presence of a broad, mildly asymmetric line from the accretion disk. The blue wing component (6.5–7.0 keV) instead is likely a blend of different contributions, and appears to be constant when

Figure 18. ***XMM Measures Accretion Disk Hot Spots.*** *(Top three panels) Nardini et al. (2016) excess emission map in the Fe K band with a resolution in the energy–time plane of 100 eV × 5 ks. The image is smoothed with an elliptical Gaussian kernel with FWHM of 250 eV × 15 ks. Energies are in the observed frame. (Bottom) The Fe K emission complex in three 30 ks intervals corresponding to states of: quiescence (dots; 10–40 ks), red flare (crosses; 75–105 ks), and blue flare (diamonds; 253–283 ks). Significant changes on short timescales appear on both sides of the narrow 6.4 keV line (green), locating the origin of the broad component(s) from the inner accretion disk.*

integrated over long enough exposures. However, the Fe K excess emission map (**Figure 18**) computed over the 7.5 days of the XMM monitoring shows that both the red and blue features are actually highly variable on timescales of ~10–15 hours in an uncorrelated fashion, suggesting that they might arise from short-lived hotspots on the disk surface, located within a few tens of gravitational radii from the central supermassive black hole and possibly illuminated by magnetic reconnection events.

Outflows and feedback (winds and jets): **King** *et al.* (2017) investigated the nature of the disk/corona/jet connection in AGN, presenting an in-depth look at the jet and coronal properties of 41 AGN based on NuSTAR, XMM, and NVSS 1.4 GHz data. They find that the radio Eddington luminosity scales inversely with X-ray reflection fraction, and scales directly with the distance between the corona and the reflected regions in the disk. Spectral modeling indicates that the corona is outflowing and propagates into the large-scale jet. **King** *et al.* predict that the model describes the data well and predicts that the corona has mildly relativistic velocities, v ~ 0.04–0.4c. They also postulate that the corona must be "far" from the disk such that the path length measured from the time-lags are close to the corona's height above the disk, and that the inner disk becomes radiation-pressure-dominated just before the AGN becomes "radio-loud." The last point suggests that a thick inner disk is needed to efficiently collimate and accelerate jets in AGN due to the large-scale height of the region that is dominated by radiation pressure.

Combining XMM and radio data of AGN is leading to new insight into the disk/corona/jet connection in AGN.

1.4.10 Stars: Exoplanets, Star Formation, and Stellar Coronae

Exoplanets: With the discovery of Earth-sized planets in the habitable zones of late M-type dwarfs, several XMM papers appeared on this new class of exoplanets. Ribas *et al.* (2016, 2017) used Proxima Centauri's X-ray luminosity to estimate the star's effect on Proxima b, a 1.3 M_{Earth} planet at 0.05 AU. Although the planet currently receives 30 times more EUV radiation than Earth and 250 times more X-rays, they conclude that Proxima b has lost less than an Earth ocean's worth of hydrogen before reaching its habitable zone 100–200 Myr after its formation 4.8 Gyr ago. For the same star, **Wargelin** *et al.* (2017) used 22 years of archival X-ray and optical data to confirm its 83-day rotation period and found a 7.1-year activity cycle. Similarly, Wheatley *et al.* (2017) used an XMM observation of the M8 star TRAPPIST-1, which hosts at least 7 low-mass exoplanets, to model the effect of XUV emission on the atmospheric evolution of three Earth-mass exoplanets in TRAPPIST-1's habitable zone.

XMM has examined the effect of XUV emission for higher-mass G- and K-type host stars on the evaporating atmospheres of a super-Earth (Bourrier *et al.* 2017), a super-Neptune (Bourrier *et al.* 2016), and multiple hot Jupiters (Louden *et al.* 2017, Lalitha *et al.* 2018). **Detailed stellar modeling (Fontonla et al. 2016) and panchromatic spectral energy distributions (Loyd et al. 2016) of exoplanet host stars are just a few examples of the type of observations that XMM continues to do that will be essential to the success of TESS**.

XMM is contributing to our understanding of the effects of stellar X-ray activity on the habitability of planets.

Coronal Activity: To support exoplanet discoveries by TESS, CHEOPS, and WFIRST, **Hinkel** *et al.* (2017) have compiled the Catalogue of Stellar Unified Properties for 951 cool stars within 30 pc. Two recent studies have further elucidated the evolution of coronal XUV emission: **Nuñez & Argüeros** *et al.* (2016) found a shallow decline with age for young clusters (<600 Myr), while Booth *et al.* (2017) found a much steeper decline in activity with log(t) for older clusters (>1 Gyr). Akin to the Sun's 11-year activity cycle, cool stars show a remarkable range of activity cycles. For τ Böotis (F7), which hosts a hot Jup*iter,* Mittag *et al.* (2017) find a very short 4-month X-ray activity cycle, while other stars show long activity cycles: 61 Cygni A – 7.2 years (Boro Saikia *et al.* 2016) and HD 81809 – 7.3 years (Orlando *et al.* 2017).

Massive Stars: Massive stars emit X-rays via mass loss and supersonic shocks. In massive binaries, much of the X-ray emission is produced in a wind collision zone. For the 10% of massive stars with strong magnetic fields, the X-rays are produced by magnetic confinement of the wind. Time-resolved XMM spectra are used to assess the mass-loss rate, wind speed, and orbital dynamics. From 2016–2018, 26 refereed papers have appeared based on XMM observations of individual massive stars.

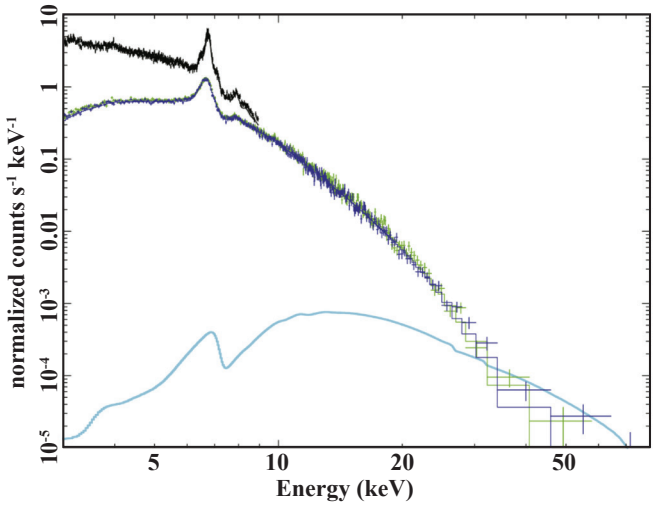

Figure 19. ***XMM's Excellent Synergy with NuSTAR.*** *XMM EPIC (top) and NuSTAR FPMA/FPMB (middle) spectra of n Car with the best-fitting thermal model (***Hamaguchi** *et al. 2016). The blue curve beneath shows the power law component measured from a prior Suzaku observation.*

Understanding mass loss is essential for understanding the evolution of massive stars, and thus our understanding of supernova progenitors. The 100 $M_\odot$ LBV η Carinae is a colliding wind system with a 5.5-year orbit. **Hamaguchi** *et al.* (2016) and **Corcoran** *et al.* (2017) observed the system with XMM, NuSTAR, and Swift through periastron passage in 2014, detecting X-ray emission up to 50 keV (**Figure 19**). The column density to the hotter 6 keV thermal component during the deep dip around periastron reached $N_H \approx 10^{24}$ cm^{-2}, the highest ever measured.

Future Stellar Research: XMM observations will yield further insights on the effect of XUV radiation on protoplanetary disks and exoplanet atmospheric evaporation. This is of particular importance when combined with the current TESS mission and the upcoming launch of JWST. XMM will continue to monitor late-type stars to better understand X-ray activity cycles, magnetic dynamos, and the evolution of XUV emission. XMM will observe massive stars, including the Gamma Cas stars, magnetic massive stars and colliding wind binaries, not only to understand their underlying emission mechanisms, but also to help understand mass loss and evolution.

For η Carinae, XMM is crucial for reliably tracking its absorption variation measured from the 1–5 keV band and measuring the hottest plasma temperature mainly using the Fe K emission lines. The next periastron is coming in February 2020. Optical studies suggest a gradual decline of line of sight absorption for decades, and a comparison to the X-ray absorption using XMM would be important.

XMM can be used in tandem with NuSTAR to constrain the hard X-ray emission from the most massive stars, such as η Carinae (**Figure 19**).

1.4.11 Supernovae/Supernova Remnants

XMM's combination of good sensitivity and spatial resolution is key for studies of SNR. Information about the mechanisms of SNR explosions, SN ejecta, interactions with nearby molecular clouds, and SN progenitors are fundamental to understanding their nature.

A high priority for such studies is the mechanism of supernova explosions, including the origin of neutron star kicks. Katsuda *et al.* (2018) used XMM and Chandra data in a study of six young core-collapse remnants to show that the intermediate mass ejecta are expelled in opposition to the measured NS motions. This supports a hydrodynamical origin for the kicks, as opposed to anisotropies in the neutrino emission.

XMM can detect soft line emission from elements such as nitrogen, that uniquely probes SNR interactions with the environment (molecular clouds, circum- vs. interstellar).

Basic insights are also sought for the type of supernova that produces a given SNR. Katusda *et al.* (2015a) used data including the RGS to support the inference that the historical Kepler's SN was an overluminous Type Ia (SN1991T-like). The relative ejecta abundances for the remnant are similar to those for the established overluminous Ia SNR 0509-67.5 rather than to more standard Ia events. Information about SNR ejecta is found in older remnants as well. Garcia *et al.* (2017) identified outlying ejecta fragments ("shrapnel") in the aged Vela remnant that are arranged opposite each other in a jet-like geometry. In the non-thermal X-ray dominated SNR, RXJ1713.7-3946, XMM revealed previously undetected line emission, with element abundances implying an origin in the ejecta and a SN progenitor of relatively low mass (Katsuda *et al.* 2015b).

The XMM long program deep exposure of SN1006 (**Figure 20**) shows the true power of XMM for spatially-resolved spectroscopy for bright sources.

XMM data were the focus of two doctoral dissertation studies of SNRs in external galaxies. Maggi *et al.* (2016) created the first homogenous X-ray catalog of remnants in the LMC, particularly identifying SNRs with ejecta emission and also Fe K emission. They make the most complete assessment to date of the relative populations of Ia and core-collapse events in the LMC, and show that the X-ray luminosity function has an excess of bright sources compared to other galaxies in the Local Group. For M33, **Garofali** *et al.* (2017) analyzed known and new SNRs at radio, optical and X-ray wavelengths. They conclude that differences between the X-ray luminosity function and that of the LMC are more strongly affected by star formation history and local environment than by metallicity effects.

Certain individual SNRs continue to attract intensive study. A comprehensive spatially-resolved spectral study was made using LP data for SN1006, highlighting mixing in both the ejecta and swept-up ISM (**Li** *et al.* 2016; **Figure 20**), and the spatially varying properties of the nonthermal emission (**Li** *et al.* 2018b). An asymmetric explosion of the progenitor star is needed to explain the asymmetric ejecta distribution. To further examine progenitors, the rapid late-time mass-loss histories of Type IIn progenitors were examined through studies of their X-ray and radio light curves (SN2005kd: **Dwarkadas** *et al.* 2016). **Given large variations from event to event, it seems increasingly likely that SNe IIn may arise from more than one progenitor type**.

Doroshenko *et al.* (2017) performed the first spatially resolved X-ray spectral analysis of the complete shell of HESS J1731−347. The correlation of X-ray absorption with CO indicates that the remnant is interacting with a nearby molecular cloud. XMM also provides a shock velocity for the southeastern region of RX J1713.7−3946, where the the remnant is expanding into the original ambient medium (Acero *et al.* 2017). If this medium is uniform, the remnant age is consistent with historical records for SN 393. **The proper motion measurement was uniquely possible with XMM given the low surface brightness and large extent of the remnant**.

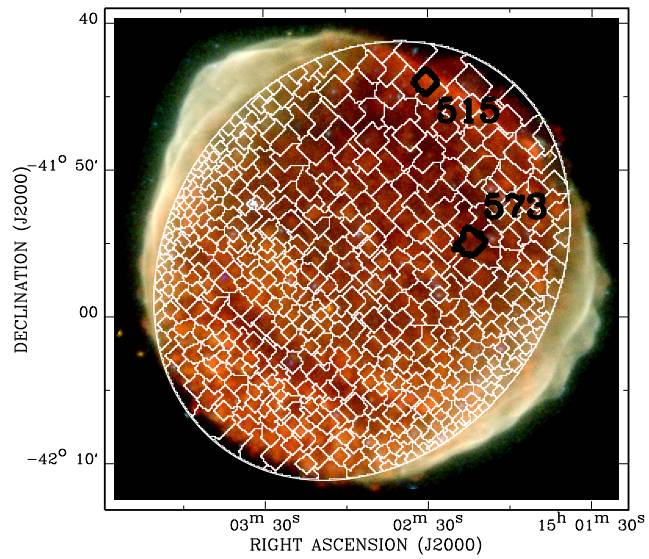

Figure 20. ***The Power of XMM's Spatially-resolved Spectroscopy!*** *583 individual spectral regions overlaid on the tricolour image of SN1006 (red: 0.3–1 keV; green:1–2 keV; blue: 2–8 keV). Each region contains >1,000 counts (***Li** *et al. 2016).*

1.4.12 The Solar System

XMM's strong soft response has long made it important to solar system studies of charge-exchange emission due to solar wind interactions and planetary auroral emission.

Jupiter: Due to its strong magnetic field and rapid rotation, Jupiter has a complex, highly energetic, and poorly understood magnetosphere. Aurorae track the location of its magnetopause and the magnetic reconnection that allows solar wind ions to be accelerated in the magnetosphere. How that acceleration occurs is not clear. A 2016 observing campaign showed that the north and south auroral zones behave very differently, and the frequencies of auroral pulsations cannot be explained (Dunn *et al.* 2017). Tantalizing early results of a multi-mission campaign in 2017–18 to observe the aurorae of Jupiter were presented at the 2017 American Geophysical Union Meeting.

Earth: XMM has just observed the Earth's magnetopause to study the SWXC. This work is being done by a member of the XMM GOF [PI: Kuntz].

A multi-mission campaign in 2017–18 with XMM, including Juno, observed Jupiter's aurorae simultaneously with *in situ* measurements of the Jovian environment.